Appendix for

Mechanism and inhibition of the papain-like protease, PLpro, of SARS-CoV-2

Theresa Klemm, Gregor Ebert, Dale J. Calleja, Cody C. Allison, Lachlan W. Richardson, Jonathan P. Bernardini, Bernadine G. C. Lu, Nathan W. Kuchel, Christoph Grohmann, Yuri Shibata, Zhong Yan Gan, James P. Cooney, Marcel Doerflinger, Amanda E. Au, Timothy R. Blackmore, Gerbrand J. van der Heden van Noort, Paul P. Geurink, Huib Ovaa[#], Janet Newman, Alan Riboldi-Tunnicliffe, Peter E. Czabotar, Jeffrey P. Mitchell, Rebecca Feltham, Bernhard C. Lechtenberg, Kym N. Lowes, Grant Dewson, Marc Pellegrini[*], Guillaume Lessene[*] and David Komander[*]

[#] deceased

* Correspondence to David Komander, dk@wehi.edu.au ; Guillaume Lessene, glessene@wehi.edu.au ; Marc Pellegrini, pellegrini@wehi.edu.au

Table of Contents:

Appendix Figure S1

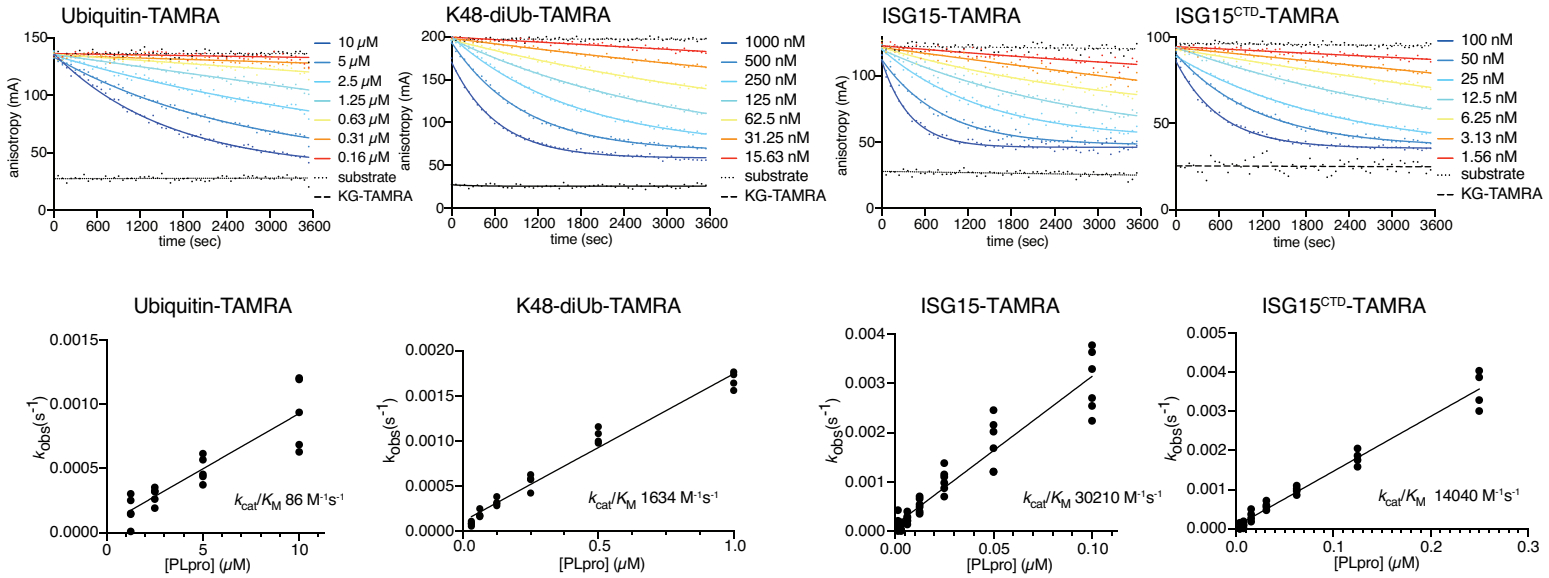

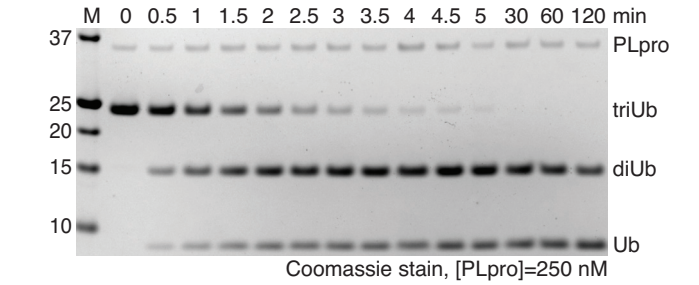

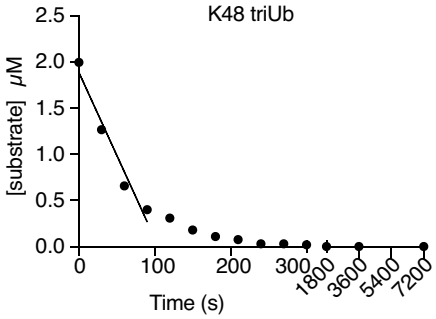

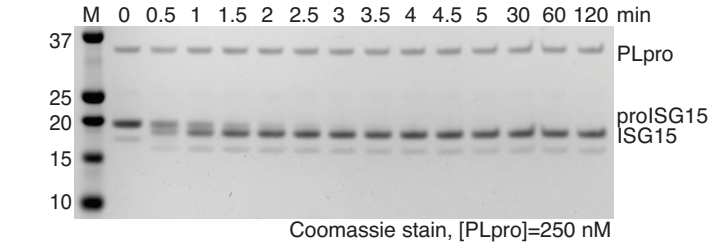

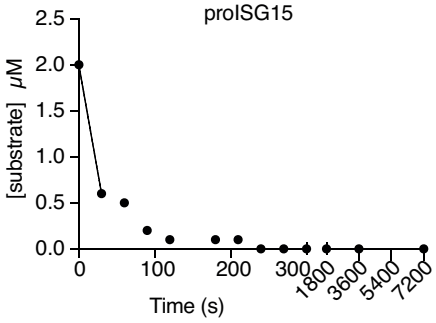

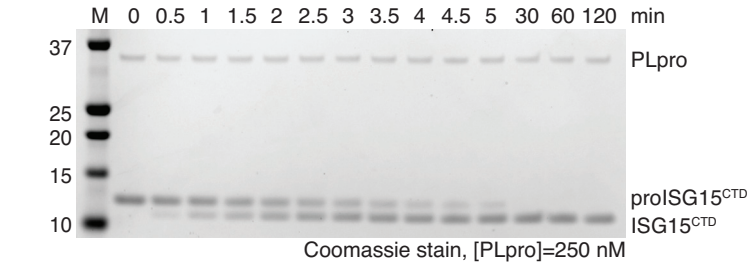

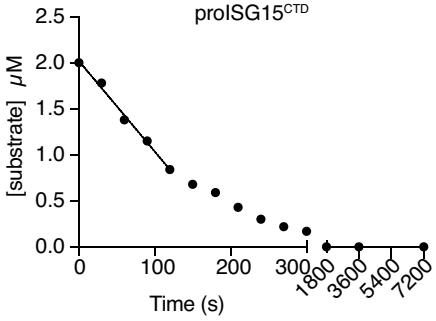

Appendix Figure S1 – Gel-based kinetics and catalytic efficiency.

A) Raw data plots (*top,* one experiment shown) was used to calculate catalytic efficiency (k_{cat}/K_M) (*bottom*). Experiments were performed in technical triplicate and n=5 (Ub-TAMRA), n= 6 (ISG15-TAMRA), n=4 ($ISG15^{CTD}$-TAMRA, K48-diUb-TAMRA) biological replicates. See **Methods** for further details.

B) In order to quantify SARS2 PLpro activity in an alternative way, triubiquitin cleavage was followed over a time course, resolved on Coomassie-stained SDS-PAGE gels. The disappearance of triubiquitin was quantified by densitometry, plotted to the right. The linear part of the data, corresponding to an estimated observed catalytic rate (k_{obs}), is indicated by a line.

C, D) For direct comparison, hydrolysis of extended 'pro'-forms of human ISG15, in which the modifier is extended by 8 residues on the C-terminus, to the mature form sporting a free Gly156-Gly157 C-terminus, was analysed as in **B,** as previously described (Swatek *et al*, 2018). The loss of 8 residues can be visualised as a small shift in size by SDS-PAGE. Disappearance of the higher molecular weight band was quantified by densitometry and plotted on the right. The linear part of the curve was used to visually indicate k_{obs}. Experiments were performed in duplicate.

Since identical enzyme concentrations (250 nM) were used in this assay, k_{obs} is comparable between experiments in **B-D**; however, the difference between cleaving a triubiquitin with an isopeptide linkage and an S1'-ubiquitin moiety, and cleaving a linear peptide off the C-terminus of ISG15, may lead to differences in PLpro activity.

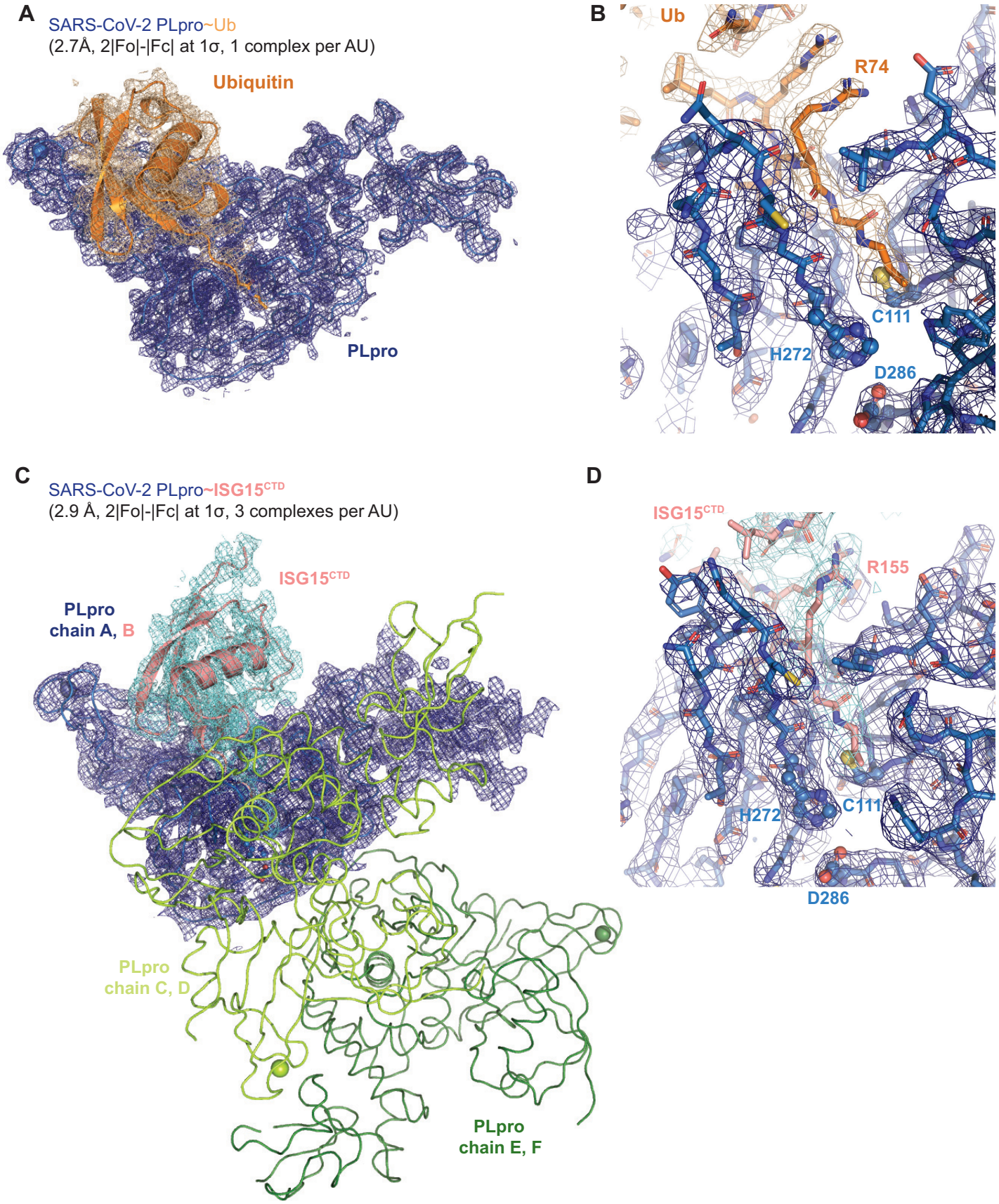
A
SARS-CoV-2 PLpro~Ub
(2.7Å, 2|Fo|-|Fc| at 1σ, 1 complex per AU)
Ubiquitin
PLpro
B
Ub
R74
C111
H272
D286
C
SARS-CoV-2 PLpro~ISG15CTD
(2.9 Å, 2|Fo|-|Fc| at 1σ, 3 complexes per AU)
ISG15CTD
PLpro
chain A, B
PLpro
chain C, D
PLpro
chain E, F
D
ISG15CTD
R155
H272
C111
D286

Appendix Figure S2. Electron density for PLpro complexes

A) 2|Fo|-|Fc| electron density, contoured at 1σ, for the SARS2 PLpro~Ub complex. The full asymmetric unit is shown. SARS2 PLpro is shown as a ribbon, and ubiquitin is shown in cartoon representation.

B) Detailed electron density for the ubiquitin C-terminal tail in the active site, with the propargyl linked to catalytic Cys111.

C) 2|Fo|-|Fc| electron density, contoured at 1σ, for the SARS2 PLpro~ISG15^{CTD} complex covering chain A (PLpro, ribbon) and B (ISG15^{CTD}, cartoon). The remainder (chains C-F) of the asymmetric unit are shown as a ribbon without map.

D) Detailed electron density for the ISG15 C-terminal tail in the active site, with the propargyl-linked to catalytic Cys111.

Appendix Table S1. High Throughput Screening Table.

Category	Parameter	Description
Assay	Type of assay	Enzymatic, endpoint
	Target	SARS-CoV-2 Papain-like Protease
	Primary measurement	Fluorescence intensity
	Key reagents	Ub-Rhodamine
Library	Library size	5,576 compounds
	Library composition	Small molecule, including FDA-approved drugs, advanced preclinical compounds and focused sets.
	Source	Commercial and in-house curated collections (see Methods)
Screen	Format	1536 well plate
	Concentration tested	4.2 µM in 2% DMSO
	Plate controls	Negative control; 2% DMSO, positive control; compound rac5c (see manuscript, Figure 5)
	Reagent/ compound dispensing system	See Methods
	Detection instrument and software	PHERAstar FSX (BMG)
	Assay validation/QC	Robust Z' > 0.5
	Hit criteria	>4*MAD above negative control
	Hit rate	0.45%
Post-HTS analysis	Counter screen	Human USP21, Ub-Rhodamine
	Additional assay(s)	
	Confirmation of hit purity and structure	LC/MS

Appendix Supplementary Methods - Compound synthesis and characterisation

General chemistry

Anhydrous solvents were obtained commercially (SIGMA-ALDRICH, Missouri, USA) and used without further purification. All other commercial reagents were used as supplied. All non-aqueous reactions were performed in oven-dried glassware under inert atmosphere (nitrogen gas), unless otherwise specified. Analytical thin-layer chromatography was performed on silica gel $60F_{254}$ aluminium-backed plates (MERCK MILLIPORE) and were visualised by fluorescence quenching under UV light or by $KMnO_4$ staining. Chromatography was performed with silica gel 60 (particle size 0.040 – 0.063 µm) using an automated purification system (ISCO TELEDYNE). NMR spectra were recorded on a Bruker Ascend-300 300 MHz at 298 K unless otherwise specified. Chemical shifts are reported in ppm on the δ scale and referenced to the appropriate solvent peak. DMSO-d_6, CD_3OD and $CDCl_3$ contain H_2O (*J* refers to coupling constant; s: singlet, d: doublet, t: triplet, q: quadruplet, m: multiplet, dq: doublet of quadruplets). HRMS analyses were carried out at the Monash University Mass Spectrometry Facility on an Agilent 6224 TOF LC/MS Mass Spectrometer coupled to an Agilent 1290 Infinity (Agilent, Palo Alto, CA). All data were acquired, and reference mass corrected via a dual-spray electrospray ionisation (ESI) source. LCMS were recorded on an Agilent LCMS system composed of an Agilent G6120B Mass Detector, 1260 Infinity G1312B Binary pump, 1260 Infinity G1367E HiPALS autosampler and 1260 Infinity G4212B Diode Array Detector. Conditions for LCMS were as follows, (Method A) column: Poroshell 120 EC-C18, 2.1 x 50 mm 2.7 Micron at 20 °C, injection volume 2 µL, gradient: 5–100% B over 3 min (solvent A: water 0.1% formic acid; solvent B: acetonitrile 0.1% formic acid), flow rate: 0.8 mL/min, detection: 254 nm, acquisition time: 5 min. HPLC conditions used to assess purity of final compounds were as follows, column: Phenomenex Gemini C18, 2.0 x 50 mm; injection volume 20 µL; gradient: 0–100% Buffer B over 6 min (buffer A: 0.1% formic acid in autoclaved MilliQ water; buffer B: 0.1% formic acid in 100% acetonitrile), flow rate: 1.0 mL/min, detection: 214 or 224 nm.

Experimental – Racemic compounds

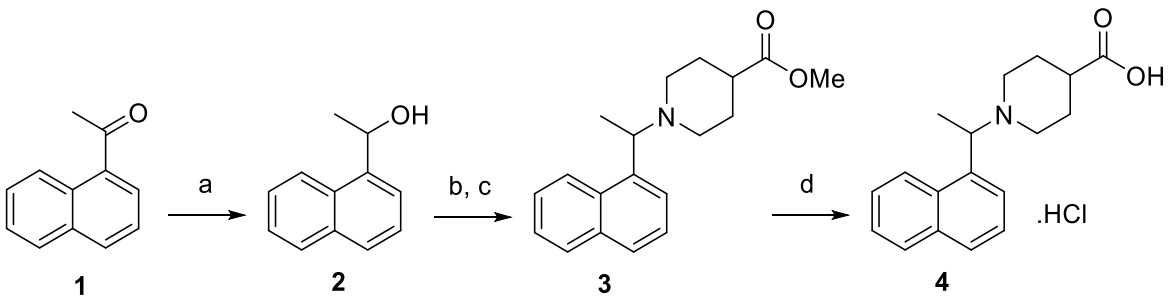

Step (a)

To a 0 °C solution of 1'-acetonaphthone (1.1 g, 6.5 mmol) in EtOH (20 mL) was added $NaBH_4$ (286 mg, 7.6 mmol) in one portion. The cooling bath was removed, and the reaction stirred until complete by LCMS. The reaction was concentrated under reduced pressure and the

crude partitioned between saturated aqueous NH_4Cl and EtOAc. The layers were separated and the aqueous further extracted with EtOAc. The combined organics were dried over anhydrous $MgSO_4$, filtered and concentrated under reduced pressure. The crude residue was subject to purification by combi-flash chromatography (0-40% EtOAc/n-heptane) to give 1-(naphthalen-1-yl)ethanol as a white solid (1.1 g, 98%).
^{1}H NMR (300 MHz, $CDCl_3$) δ 8.17 – 8.08 (m, 1H), 7.94 – 7.82 (m, 1H), 7.79 (dq, *J* = 8.2, 0.8 Hz, 1H), 7.69 (dt, *J* = 7.2, 1.0 Hz, 1H), 7.59 – 7.43 (m, 3H), 5.69 (q, *J* = 6.7 Hz, 1H), 1.98 (s, 1H), 1.68 (d, *J* = 6.4, 0.4 Hz, 3H).

Steps (b, c)
To a 0 °C solution of 1-(naphthalen-1-yl)ethanol (1.1 g, 6.4 mmol) in dry CH_2Cl_2 (20 mL) was added $SOCl_2$ (500 µL, 6.9 mmol) drop wise followed by catalytic DMF (1 drop). The reaction was stirred until complete by TLC. The reaction mixture was quenched with saturated aqueous NH_4Cl and extracted with CH_2Cl_2. The combined organics were dried over anhydrous $MgSO_4$, filtered and concentrated under reduced pressure to give the desired alkyl chloride without any further purification. The crude alkyl chloride was taken up in dry MeCN (10 mL) and sequentially was added K_2CO_3 (1.5 g, 10.8 mmol) and methyl isonipectoate (960 µL, 7.1 mmol). The reaction was stirred at 70 ºC until complete by LCMS. The reaction was concentrated under reduced pressure and the crude residue partitioned between saturated aqueous NH_4Cl and EtOAc. The layers were separated and the aqueous further extracted with EtOAc. The combined organics were dried over anhydrous $MgSO_4$, filtered and concentrated under reduced pressure. The crude residue was subject to purification by combi-flash chromatography (0-25% EtOAc/CH_2Cl_2) to give methyl 1-(1-(naphthalen-1-yl)ethyl)piperidine-4-carboxylate as a yellow oil (574 mg, 37%).
^{1}H NMR (300 MHz, $CDCl_3$) δ 8.48 – 8.39 (m, 1H), 7.90 – 7.79 (m, 1H), 7.74 (d, *J* = 8.0 Hz, 1H), 7.57 (d, *J* = 7.1 Hz, 1H), 7.54 – 7.37 (m, 3H), 4.10 (q, *J* = 6.7 Hz, 1H), 3.66 (s, 3H), 3.19 – 3.09 (m, 1H), 2.87 – 2.78 (m, 1H), 2.37 – 2.21 (m, 1H), 2.16 – 1.98 (m, 2H), 1.97 – 1.87 (m, 1H), 1.85 – 1.66 (m, 3H), 1.46 (d, *J* = 6.7 Hz, 3H).

Step (d)
To a stirred solution of methyl 1-(1-(naphthalen-1-yl)ethyl)piperidine-4-carboxylate (564 mg, 1.9 mmol) in THF/MeOH (3:2) was added 40% aqueous NaOH (1 mL). The reaction was warmed at 60 °C until complete by LCMS. The reaction was concentrated under reduced pressure and the pH adjusted to 2 with 5N HCl. The precipitated solids were collected by filtration, washed with chilled H_2O and dried to give 1-(1-(naphthalen-1-yl)ethyl)piperidine-4-carboxylic acid hydrochloride as a white solid (552 mg, 91%).
^{1}H NMR (300 MHz, CD_3OD) δ 8.30 (d, *J* = 8.6 Hz, 1H), 8.08 – 7.96 (m, 2H), 7.91 – 7.83 (m, 1H), 7.75 – 7.55 (m, 3H), 5.44 (d, *J* = 6.4 Hz, 1H), 4.03 (s, 1H), 3.29 – 3.09 (m, 2H), 2.98 (s, 1H), 2.59 (s, 1H), 2.43 – 1.62 (m, 8H).

N-(3-fluorobenzyl)-1-(1-(naphthalen-1-yl)ethyl)piperidine-4-carboxamide (rac3k)

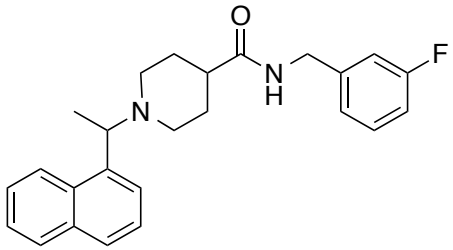

rac3k

To a solution of **4** (54 mg, 0.17 mmol) in dry DMF was added sequentially DIEA (62 mL, 0.36 mmol), ((3-fluorophenyl)methanamine (21 mL, 0.18 mmol) and HATU (71 mg, 0.19 mmol). The reaction was stirred at ambient temperature until complete by LCMS. The reaction was diluted with saturated aqueous $NaHCO_3$ and extracted with EtOAc. The combined extracts were washed with H_2O (x3) and brine, dried over anhydrous $MgSO_4$, filtered and concentrated under reduced pressure. The crude residue was subject to purification by combi-flash chromatography (0-5% MeOH/CH_2Cl_2) to give the title compound (59 mg, 90%). ^{1}H NMR (300 MHz, $CDCl_3$) δ 8.48 – 8.39 (m, 1H), 7.90 – 7.79 (m, 1H), 7.74 (d, *J* = 8.1 Hz, 1H), 7.56 (d, *J* = 7.1 Hz, 1H), 7.53 – 7.37 (m, 3H), 7.34 – 7.21 (m, 1H), 7.06 – 6.89 (m, 1H), 5.76 (s, 1H), 4.43 (d, *J* = 5.8 Hz, 2H), 4.11 (q, 1H), 3.24 (d, *J* = 11.3 Hz, 1H), 2.90 (d, *J* = 11.5 Hz, 1H), 2.26 – 1.65 (m, 7H), 1.47 (d, *J* = 6.7 Hz, 3H). ES+ MS: (M + H) 391.2. HPLC t_g = 1.5 min, >95% purity.

NMR spectra of rac3k

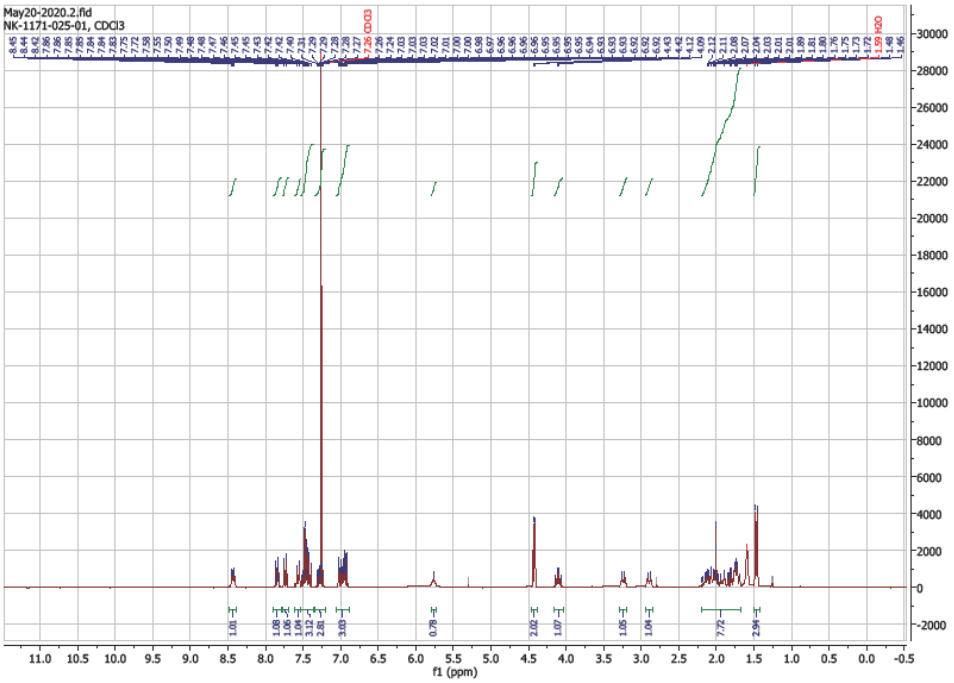

N-(4-fluorobenzyl)-1-(1-(naphthalen-1-yl)ethyl)piperidine-4-carboxamide (rac3j)

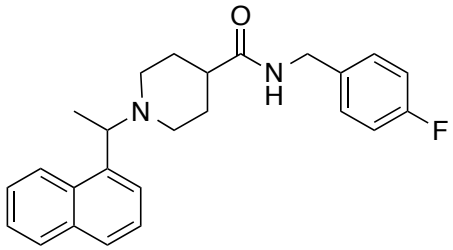

rac3j

The title compound **rac3j** was obtained as described for compound **rac3k** in 84% yield. ^{1}H NMR (300 MHz, $CDCl_3$) δ 8.42 (d, *J* = 7.8 Hz, 1H), 7.89 – 7.79 (m, 1H), 7.74 (d, *J* = 8.1 Hz, 1H), 7.56 (d, *J* = 7.1 Hz, 1H), 7.52 – 7.37 (m, 3H), 7.27 – 7.15 (m, 2H), 7.06 – 6.93 (m, 2H), 5.72 (s, 1H), 4.43 – 4.35 (m, 2H), 4.14 – 4.04 (m, 1H), 3.23 (d, *J* = 11.1 Hz, 1H), 2.89 (d, *J* = 11.4 Hz, 1H), 2.21 – 1.65 (m, 7H), 1.46 (d, *J* = 6.7 Hz, 3H). ES+ MS: (M + H) 391.2. HPLC t_g = 1.5 min, >95% purity.

NMR spectra of rac3j

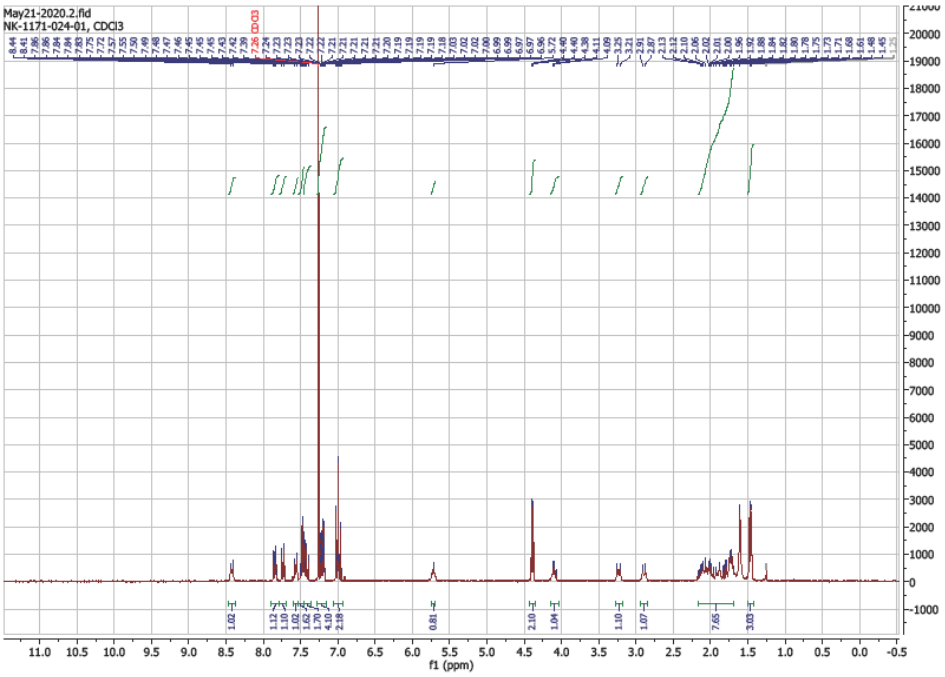

N-((2-methoxypyridin-4-yl)methyl)-1-(1-(naphthalen-1-yl)ethyl)piperidine-4-carboxamide (rac5c)

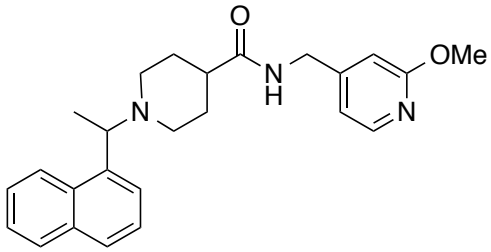

rac5c

The title compound **rac5c** was obtained as described for compound **rac3k** in 74% yield. ^{1}H NMR (300 MHz, $CDCl_3$) δ 8.41 (br s, 1H), 8.08 (d, *J* = 5.3 Hz, 1H), 7.90 – 7.81 (m, 1H), 7.75 (d, *J* = 8.2 Hz, 1H), 7.58 (s, 1H), 7.54 – 7.38 (m, 3H), 6.77 – 6.69 (m, 1H), 6.58 (s, 1H), 5.84 (s, 1H), 4.39 (d, *J* = 6.0 Hz, 2H), 4.15 (s, 1H), 3.91 (s, 3H), 3.31 – 3.21 (m, 1H), 2.98 – 2.88 (m, 1H), 2.22 – 1.71 (m, 7H), 1.55 – 1.43 (m, 3H). ES+ MS: (M + H) 404.2. HPLC t_g = 1.2 min, >95% purity.

NMR spectra of rac5c

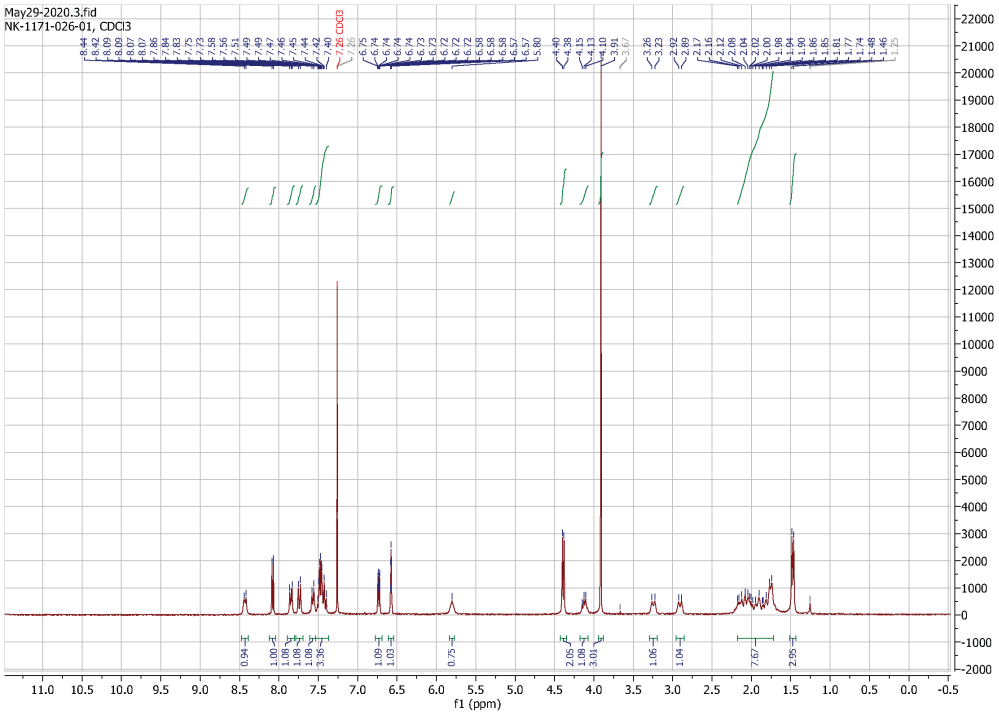

Appendix Reference

Swatek KN, Aumayr M, Pruneda JN, Visser LJ, Berryman S, Kueck AF, Geurink PP, Ovaa H, van Kuppeveld FJM, Tuthill TJ, Skern T & Komander D (2018) Irreversible inactivation of ISG15 by a viral leader protease enables alternative infection detection strategies. *Proceedings of the National Academy of Sciences* **115:** 2371–2376